FIELD ESTIMATES OF BODY DRAG COEFFICIENT ON THE BASIS OF DIVES IN PASSERINE BIRDS

ANDERS HEDENSTRÖM[1],* AND FELIX LIECHTI[2]

[1]*Department of Animal Ecology, Ecology Building, SE-223 62 Lund, Sweden* and [2]*Swiss Ornithological Institute, CH-6204 Sempach, Switzerland*

*e-mail: anders.hedenstrom@zooekol.lu.se

Summary

During forward flight, a bird's body generates drag that tends to decelerate its speed. By flapping its wings, or by converting potential energy into work if gliding, the bird produces both lift and thrust to balance the pull of gravity and drag. In flight mechanics, a dimensionless number, the body drag coefficient ($C_{D,par}$), describes the magnitude of the drag caused by the body. The drag coefficient depends on the shape (or streamlining), the surface texture of the body and the Reynolds number. It is an important variable when using flight mechanical models to estimate the potential migratory flight range and characteristic flight speeds of birds. Previous wind tunnel measurements on dead, frozen bird bodies indicated that $C_{D,par}$ is 0.4 for small birds, while large birds should have lower values of approximately 0.2. More recent studies of a few birds flying in a wind tunnel suggested that previous values probably overestimated $C_{D,par}$.

We measured maximum dive speeds of passerine birds during the spring migration across the western Mediterranean. When the birds reach their top speed, the pull of gravity should balance the drag of the body (and wings), giving us an opportunity to estimate $C_{D,par}$. Our results indicate that $C_{D,par}$ decreases with increasing Reynolds number within the range 0.17–0.77, with a mean $C_{D,par}$ of 0.37 for small passerines. A somewhat lower mean value could not be excluded because diving birds may control their speed below the theoretical maximum. Our measurements therefore support the notion that 0.4 (the 'old' default value) is a realistic value of $C_{D,par}$ for small passerines.

Key words: aerodynamics, bird, drag, flight, body drag coefficient, passerine, diving speed, migration.

Introduction

The mechanical power required for flight in birds can be calculated at different airspeeds according to a simple theory (Pennycuick, 1975; Pennycuick, 1989). For cruising flapping flight, three main power components sum to give the total mechanical power: induced power arising from the rate of work required to support the weight of the bird; profile power required to overcome the drag of the flapping wings; and parasite power required to overcome the drag of the body. Parasite drag depends on both skin friction and the pressure drag caused by the body. The skin friction drag component arises as a result of the body surface roughness and the associated viscous shearing forces tangential to the surface, while the parasite (or form) drag results from the distribution of pressure normal to the surface (e.g. McCormick, 1995). The different components of drag responsible for any of the three power components can be obtained from force measurements on mounted models in wind tunnels (Rae and Pope, 1984). Using this method, the parasite drag of bird bodies has been measured several times (Pennycuick et al., 1988; Tucker, 1990). These estimates, using dead, frozen bird bodies or models, have yielded body drag coefficients within the range 0.14–0.4.

By convention, the drag coefficient multiplied by the body frontal area yields the same drag as a flat plate with a fictitious shape having a drag coefficient of unity and exerting the same dynamic pressure in the airflow as the bird's body. It was observed that the frozen bird bodies caused turbulence in the boundary layer (Pennycuick et al., 1988), and it has been suggested that the body drag of a live, free-flying bird could be lower than that of a mounted bird body. Tucker (Tucker, 1990) measured the drag of a wingless peregrine falcon (*Falco peregrinus*) body in a wind tunnel and found a $C_{D,par}$ of 0.24, while a smooth surface model gave a $C_{D,par}$ of 0.14. Pennycuick et al. (Pennycuick et al., 1996) measured the wingbeat frequency of a thrush nightingale *Luscinia luscinia* and a teal *Anas crecca* and calculated that, to obtain a match between the speed of minimum wingbeat frequency and the aerodynamic model prediction of the minimum power speed (V_{mp}), $C_{D,par}$ would have to be 0.1 or even lower. When calculating the mechanical power required for flight, for example according to the programs of Pennycuick (Pennycuick, 1989), a realistic value for $C_{D,par}$ has to be assumed. Depending on the value used, derived properties such

as predicted speeds for minimum power and maximum range will be affected. On the basis of wingbeat frequency measurements, Pennycuick now recommends that a $C_{D,par}$ value of 0.1 should be used as a default value with his programs for birds with streamlined bodies (Pennycuick, 1999). Estimating $C_{D,par}$ is notoriously difficult, and current values should be considered as provisional until more direct measurements of the mechanical power of birds become available.

We have used a different approach to estimate $C_{D,par}$ in small passerines. During migration, some birds occasionally terminate their migratory flights by diving steeply towards the ground, where they land. We obtained measurements of such dives during routine tracking of migratory birds by means of tracking radar. The tracks of a few of these birds were measured for such a long time that the terminal speed could be estimated with some confidence. The underlying assumption is that, when the speed reaches a constant value, then the drag will balance the pull of gravity.

Theory

When gliding or diving at constant speed along a path inclined at an angle θ to the horizontal, the forces acting on a bird will be at equilibrium, i.e. there will be no net forces causing any acceleration. At any glide angle different from a completely vertical dive, some lift must be generated, which means that the wings have to be opened to some extent. In a completely vertical dive, the wings are typically folded against the body. By measuring the airspeed (V) and the angle of the flight path with respect to the horizontal during a steady dive, the lift L and drag D forces can be calculated on the basis of airspeed and sinking speed (V_s) as follows:

$$L = m\mathbf{g}[1 - (V_s/V)^2]^{1/2} , \tag{1}$$

and

$$D = \frac{m\mathbf{g}V_s}{V} , \tag{2}$$

where m is body mass and $\mathbf{g}$ is the acceleration due to gravity. Equation 2 gives the total drag acting on the bird, which can be written as the sum of three aerodynamic components as:

$$D = D_{ind} + D_{pro} + D_{par} , \tag{3}$$

where the components are the induced, profile and parasite drag, respectively. We neglected the possible effect on drag of interference between the wings and body. Induced drag represents the cost of generating lift, profile drag is the drag of the wings and parasite drag is due to skin friction and the form drag of the body. Induced drag is:

$$D_{ind} = \frac{2kL^2}{\pi\rho b^2 V^2} , \tag{4}$$

where k is the induced drag factor (the efficiency of the wing in generating lift; ideally $k=1$, for a wing with perfect elliptical lift distribution), L is lift (equation 1), ρ is air density, b is

wingspan and V is airspeed along the glide/dive path. Profile drag is:

$$D_{pro} = \tfrac{1}{2}\rho V^2 S_w C_{D,pro} , \tag{5}$$

where S_w is the wing area and $C_{D,pro}$ is a dimensionless drag coefficient. Parasite drag is:

$$D_{par} = \tfrac{1}{2}\rho V^2 S_b C_{D,par} , \tag{6}$$

where S_b is the body frontal area of the bird and $C_{D,par}$ is the body drag coefficient, i.e. the parameter that we ultimately wish to estimate. $C_{D,par}$ is a function of Reynolds number Re (see below). By substituting equations 2 and 4–6 into equation 3 and rearranging, the body drag coefficient can be calculated as:

$$C_{D,par} = \frac{1}{S_b}\left(\frac{2m\mathbf{g}V_s}{\rho V^3} - S_w C_{D,pro} - \frac{4kL^2}{\pi\rho^2 b^2 V^4}\right). \tag{7}$$

In a vertical dive with completely folded wings, $V_s=V$, $S_w=0$ and $L=0$, and hence the body drag coefficient becomes $C_{D,par}=2m\mathbf{g}/(\rho S_b V^2)$, which is simply equation 6 rearranged; the only aerodynamic force arises from the drag of the body. To estimate $C_{D,par}$ for birds diving vertically with folded wings would be desirable since this involves a minimum number of assumptions. However, most birds tracked by radar showed inclined dives, so equation 7 has to be used. The bird tail (Thomas, 1993) and/or body can generate some lift, as indicated from measurements of zebra finches *Taenopygia guttata* (Tobalske et al., 1999), but there is no established way of estimating the lift and the associated induced drag for the body and tail. We will therefore assume that the wings are responsible for the lift causing the inclined dive angles. By assuming realistic values for the variables of equation 7 and measuring the terminal airspeed of gliding dives, we were able to estimate $C_{D,par}$.

Calculating the drag

The total lift and drag were estimated for each bird track using equations 1 and 2. From the lift, we calculated the wing area needed to generate the lift from the relationship $L=\tfrac{1}{2}\rho V^2 S_w C_L$, assuming a lift coefficient, C_L, of 0.5 (see Pennycuick, 1968). We investigated the effect of varying the values of the lift coefficient by ±50% to investigate the sensitivity of the results to assumptions. When the wings are flexed, the mean chord remains almost constant (Rosén and Hedenström, 2001), and this was used to calculate an effective wingspan associated with the wing area required. Here, we assumed that only the wings generate any useful lift force. The mean chord of the wing c was calculated as $c=S_{max}/b_{max}$, where S_{max} is the wing area and b_{max} is the span when the wings are in the fully outstretched position. For the profile drag coefficient, we assumed $C_{D,pro}=0.014$ (Pennycuick, 1989), but we also investigated the effects of varying $C_{D,pro}$ by ±50% around this default value. Pennycuick et al. (Pennycuick et al., 1992) found a mean value of 0.02 for the wing of a Harris' hawk (*Parabuteo unicinctus*), but also lower values in the neighbourhood of 0.014. The body frontal area, which is the

reference area when calculating the parasite drag, was calculated on the basis of body mass m as $S_b=0.00813m^{0.666}$ (Pennycuick, 1989). When calculating the drag components, we used the calculated air density for the relevant mid-point altitude of each dive (US standard atmosphere; Lide, 1997).

Reynolds number

The Reynolds number Re is a dimensionless index describing the relative importance of inertial and viscous forces; it is calculated as $Re=Vl/\nu$, where V is airspeed, l is a characteristic length and ν is the kinematic viscosity of air, defined as dynamic viscosity divided by density (see Batchelor, 1967; for examples of drag and Re relevant to biology, see Vogel, 1994). We calculated Re using the diameter of the body frontal area as the reference length. Dynamic viscosity μ (Pa s) was estimated for the relevant dive midpoint altitude for each track according to the equation $\mu=1.79\times10^{-5}-(3.32\times10^{-10})Z$, where Z is altitude (data from Lide, 1997). Air density estimated for the relevant altitude was used when calculating the kinematic viscosity ν.

Materials and methods
Study sites

Bird migration was studied by tracking radar during spring 1997 in an area of the Western Mediterranean (from 19 March to 26 May). One site was situated on Mallorca, the largest of the Balearic islands, close to the southern tip of the island approximately 2 km from the coast (3°4′E, 39°18′N; 10 m above sea level). A second observation site was on the southern coast of Spain, approximately 25 km east of Malaga, 100 m inland from the east–west oriented coastline (4°8′W, 36°44′N, 20 m above sea level). Birds arriving on Mallorca had flown at least 300 km across the open sea, whereas from the north African coast to Malaga they had covered approximately 170 km.

Data collection and analysis

At both sites, flight paths of individual birds were recorded by an X-band tracking radar of the type 'Superfledermaus' (for details of the characteristics of this type of radar, see Bruderer, 1997). The fluctuation of the echo-signature, representing the wingbeat pattern of the bird, was continuously digitised, whereas the spatial position of the tracked birds (X, Y and Z coordinates) was automatically saved every second. Wingbeat frequency was analysed by selecting parts of a flight path with a low noise level and a clear wingbeat pattern and then determining the wingbeat frequency using Fast Fourier transformation analysis. For this study, we selected tracks consisting of two obviously different flight conditions. In one part (generally at the beginning of the track), wingbeat frequency had to be clearly identifiable, whereas in the other part sinking rate had to be greater than 20 m s⁻¹ over a period of at least 20 s. From these segments of rapid descent, we selected the parts with a

maximum sinking rate over at least 4 s to represent maximum diving speeds. In total, 16 tracks from Malaga and 23 from Mallorca were selected for analysis (Table 1). All dives were tracked during the day.

To match a specific wingbeat frequency to a species, we used the abundance of migratory species monitored at least every second day in the area surrounding the radar stations. In addition, almost all targets were observed and classified visually by a telescope mounted parallel to the radar antenna. Unfortunately, exact species identification was not possible because of the large distances (at least several hundred metres), but all tracks included in this study refer to passerine birds. The observers detected no signs of flapping wings when the birds were diving, indicating that diving birds held their wings motionless and did not supply any additional power. No signs that the legs were held in an outstretched position, causing extra drag, were observed, although this could have been difficult to detect.

To calculate air density, air pressure and temperature at the bird's flight altitude, data were taken from the radio-sonde measurements at Gibraltar (for the Malaga site) and Palma de Mallorca (12 h UTC). Wind profiles were collected every 4 h at the study sites by tracking helium-filled balloons by radar up to 4000 m above sea level. To calculate horizontal air speed and diving angle, the flight path of the balloon between the height at the start and end of the dive was subtracted from the bird's flight path. Calculations were performed incorporating the wind data from the measurements before and after the track of the dive. According to these two measurements, diving angle for an individual bird differed maximally by 12° (mean 3.8°) and horizontal air speed by 7 m s⁻¹ (2.4 m s⁻¹). In seven cases, data from only one wind measurement were available.

Body mass and wing morphology

It was impossible to obtain data on body mass and wing morphology for those individuals tracked by radar. Information was therefore obtained from Pennycuick (Pennycuick, 1999) and from our own unpublished database for the species that were likely candidates on the basis of the wingbeat signatures obtained prior to the commencement of dives. Species and morphological data used for the calculations are shown in Table 2.

Results
General patterns of dives

Information for each tracking is given in Table 1. All tracks included in this analysis refer to rapid descents from cruising altitudes during migration of up to 3700 m above sea level to relatively low altitudes. Most descents probably refer to the termination of migratory flights, although a few may include birds that continued the flight at a lower altitude. A few examples of dive patterns are shown in Fig. 1, in which altitude is plotted with respect to time. For example, bird 267 descended from almost 3500 m to approximately 1200 m in

Table 1. *Data for 39 tracks of diving birds used to estimate body drag coefficients*

Species	No.	ρ (kg m^{-3})	Z_1 (m)	Z_2 (m)	Δt (s)	V_s (m s^{-1})	θ (degrees)	V (m s^{-1})	$C_{D,par}$
Wheatear	378	1.06	1051	894	4	39.3	83.3	39.5	0.41
Wheatear	268	1.16	716	265	15	30.1	69.8	32.0	0.54
Meadow pipit	212	1.19	258	141	4	29.3	61.7	33.2	0.42
Meadow pipit	342	1.15	425	330	4	23.8	52.4	30.0	0.50
Nightingale	283	1.16	619	368	8	31.4	60.4	36.1	0.37
Nightingale	319	1.14	942	686	9	28.4	67.9	30.7	0.56
Nightingale	320	1.11	732	607	5	25.0	61.1	28.6	0.63
Barn swallow	267	1.00	2930	2722	4	52.0	83.5	52.3	0.23
Barn swallow	231	1.07	1301	97	32	37.6	74.7	39.0	0.37
Robin	304	1.09	1354	1216	4	34.5	63.8	38.4	0.35
Yellow wagtail	336	1.04	2891	2728	4	40.8	64.0	45.3	0.26
Yellow wagtail	217	1.17	981	821	4	40.0	78.5	40.8	0.31
Yellow wagtail	236	0.99	2347	2035	8	39.0	75.8	40.2	0.38
Yellow wagtail	352	1.11	3060	2910	4	37.5	66.6	40.9	0.31
Yellow wagtail	242	1.15	1865	1644	6	36.8	58.2	43.3	0.24
Yellow wagtail	250	1.09	1764	1547	6	36.2	65.6	39.7	0.33
Yellow wagtail	221	1.16	1510	1375	4	33.8	75.8	34.8	0.43
Yellow wagtail	250	1.08	1987	1793	6	32.3	66.3	35.3	0.42
Yellow wagtail	276	1.12	654	425	8	28.6	72.8	30.0	0.59
Yellow wagtail	336	1.10	1026	927	4	24.8	50.9	31.9	0.43
Spotted flycatcher	297	1.05	3500	3042	10	45.8	59.6	53.1	0.17
Spotted flycatcher	312	1.18	629	547	4	20.5	59.5	23.8	0.77
Redstart	279	1.13	1540	1358	5	36.4	58.9	42.5	0.25
Redstart	289	1.12	1882	1742	4	35.0	55.7	42.4	0.24
Redstart	347	1.12	1409	1279	4	32.5	70.9	34.4	0.42
Reed warbler	232	1.18	691	561	4	32.5	77.2	33.3	0.41
Pied flycatcher	290	0.89	2498	2311	4	46.8	60.6	53.7	0.19
Pied flycatcher	335	1.18	689	545	4	36.0	66.4	39.3	0.28
Pied flycatcher	314	1.05	2558	2273	8	35.6	56.2	42.9	0.24
Pied flycatcher	314	1.16	542	400	4	35.5	72.0	37.3	0.32
Pied flycatcher	340	1.17	809	466	10	34.3	71.3	36.2	0.34
Pied flycatcher	281	1.15	322	211	4	27.8	74.3	28.8	0.55
Serin	282	1.15	224	87	4	34.3	54.0	42.3	0.21
Willow warbler	215	1.06	1791	1572	6	36.5	54.6	44.8	0.19
Willow warbler	209	1.11	2448	2303	4	36.3	71.3	38.3	0.29
Willow warbler	325	1.15	914	796	4	29.5	63.7	32.9	0.35
Willow warbler	229	1.18	427	315	4	28.0	57.8	33.1	0.32
Willow warbler	325	1.16	525	422	4	25.8	50.1	33.6	0.29
Goldcrest	332	1.13	931	826	4	26.3	75.1	27.2	0.49

No. indicates the identification number for the track, ρ is estimated air density at the midpoint altitude $[(Z_1+Z_2)/2]$, Z_1 is the altitude at which the dive starts, Z_2 is the altitude at which the dive segment stops both measured as metres above ground level, Δt is the duration of the dive of maximum speed, V_s is vertical sinking speed, θ is dive angle with respect to the horizontal, V is dive speed along the dive path and $C_{D,par}$ is the estimated body drag coefficient.

Species refer to the 'best guess' according to wingbeat signature (see Materials and methods).

Scientific names are given in Table 2.

80 s, but the descent was interrupted a few times during this period (Fig. 1A). The mean rate of descent ($29.9\,\mathrm{m\,s^{-1}}$) was therefore lower than the instantaneous maximum speed ($52.3\,\mathrm{m\,s^{-1}}$) achieved over at least 4 s. This pattern of 'stepwise' descent was also evident in other birds, e.g. 232 and 352 (Fig. 1C,D), while others showed rather continuous and uninterrupted descents. Gliding/diving angles varied from 50° to a near vertical dive of 83.5°. There was no significant relationship between maximum speed along the flight path and dive angle (analysis of covariance, ANCOVA, $F_{1,25}$=0.44, P=0.51; Fig. 2). Species category had no significant effect on speed ($F_{12,25}$=0.87, P=0.58), while the effect of body mass was marginally significant ($F_{1,25}$=4.18, P=0.051). The maximum speeds ranged from 23.8 to $53.7\,\mathrm{m\,s^{-1}}$ with a mean value of $37.5\pm6.9\,\mathrm{m\,s^{-1}}$ (mean ± S.D., N=39) There was a positive relationship between the height at the middle of the dive

Table 2. *Body mass, body frontal area and wing morphology used to estimate the aerodynamic properties of the birds tracked by radar*

Species	m (kg)	S_b (cm²)[a]	b_{max} (m)	S_{max} (m²)	Chord (m)
Wheatear					
Oenanthe oenanthe L.	0.0232	6.6	0.264	0.01366	0.052
Meadow pipit					
Anthus pratensis L.	0.0199	6.0	0.273	0.0143	0.052
Nightingale					
Luscinia megarhynchos Brehm	0.0197	6.0	0.221	0.01059	0.048
Barn swallow					
Hirundo rustica L.	0.0182	5.6	0.328	0.01446	0.044
Robin					
Erithacus rubecula L.	0.0182	4.6	0.224	0.01026	0.046
Yellow wagtail					
Motacilla flava L.	0.0176	5.5	0.248	0.01051	0.042
Spotted flycatcher					
Muscicapa striata Pallas	0.0153	5.0	0.262	0.01209	0.046
Redstart					
Phoenicurus phoenicurus L.	0.015	5.0	0.2	0.01006	0.050
Reed warbler					
Acrocephalus scirpaceus Hermann	0.0123	3.9	0.2	0.00779	0.039
Pied flycatcher					
Ficedula hypoleuca Pallas	0.012	4.4	0.2	0.00873	0.044
Serin					
Serinus serinus L.	0.0114	3.9	0.214	0.00828	0.039
Willow warbler					
Phylloscopus trochilus L.	0.0087	4.0	0.194	0.00768	0.040
Goldcrest					
Regulus regulus L.	0.0054	3.5	0.146	0.00504	0.035

[a]Calculated as $S_b=0.00813m^{0.666}$ (Pennycuick, 1989).

m, body mass; S_b, body frontal area; S_{max}, maximum wing area; b_{max}, maximum wingspan; C, mean wing chord.

and the speed (ANCOVA, $F_{1,25}=43.2$, $P<0.001$). A simple regression indicated that dive speed increases by approximately 5.7 m s⁻¹ per 1000 m altitude.

Estimating the body drag

The calculated body drag coefficients ($C_{D,par}$) for all trackings of diving birds are given in Table 1. The mean estimated $C_{D,par}$ was 0.37 ± 0.13 (mean ± S.D., $N=39$), ranging from 0.17 to 0.77. We changed the assumed value for C_L (0.5) by ±50 %, but this had a negligible effect (±0.3 %) on the estimated mean $C_{D,par}$. The assumed value for $C_{D,pro}$ (0.014) was also changed by ±50 %, which again had a very small effect (±0.15 %) on the estimated $C_{D,par}$. We will therefore use the baseline assumptions for further analyses in this paper. The estimated $C_{D,par}$ showed a positive relationship with body mass, but the relationship was not statistically significant (ANCOVA, $F_{1,25}=3.60$, $P=0.069$). There was no significant relationship between $C_{D,par}$ and diving angle (ANCOVA, $F_{1,25}=1.50$, $P=0.23$). Our estimates of $C_{D,par}$ did, however show a negative relationship with the Reynolds number (Fig. 3; ANCOVA, $F_{1,25}=329.3$, $P<0.001$). The lowest values of $C_{D,par}$ of approximately 0.2 were obtained in the range of Re from 57 000 to 84 000 (Fig. 3). The linear regression equation between $C_{D,par}$ and Re was $C_{D,par}=0.82-(7.5\times10^{-6})Re$; when two data points where $C_{D,par}>0.6$ were excluded, the regression was $C_{D,par}=0.70-(5.8\times10^{-6})Re$.

Bird 267 is of particular interest; it dived almost vertically in a stepwise manner ($\theta=83.5°$) and reached a maximum speed V of 52.3 m s⁻¹ (Fig. 1A). This bird showed the wingbeat pattern typical of the barn swallow *Hirundo rustica*, which makes this observation especially valuable. The nearly vertical dive means that the wings were almost completely folded and, hence, the estimated $C_{D,par}$ of 0.23 is probably quite a reliable estimate for this bird. However, two other birds with near-vertical dives ($\theta=83.3°$ and $\theta=77.2°$) both showed an estimated $C_{D,par}$ of 0.41, which makes us suspect that they might have been braking using partially opened wings or by holding their legs/feet outstretched, although this could not be seen by the observer (see below). These two birds (378 and 232; see Table 1) reached maximum speeds of only 39.5 m s⁻¹ and 33.3 m s⁻¹, respectively.
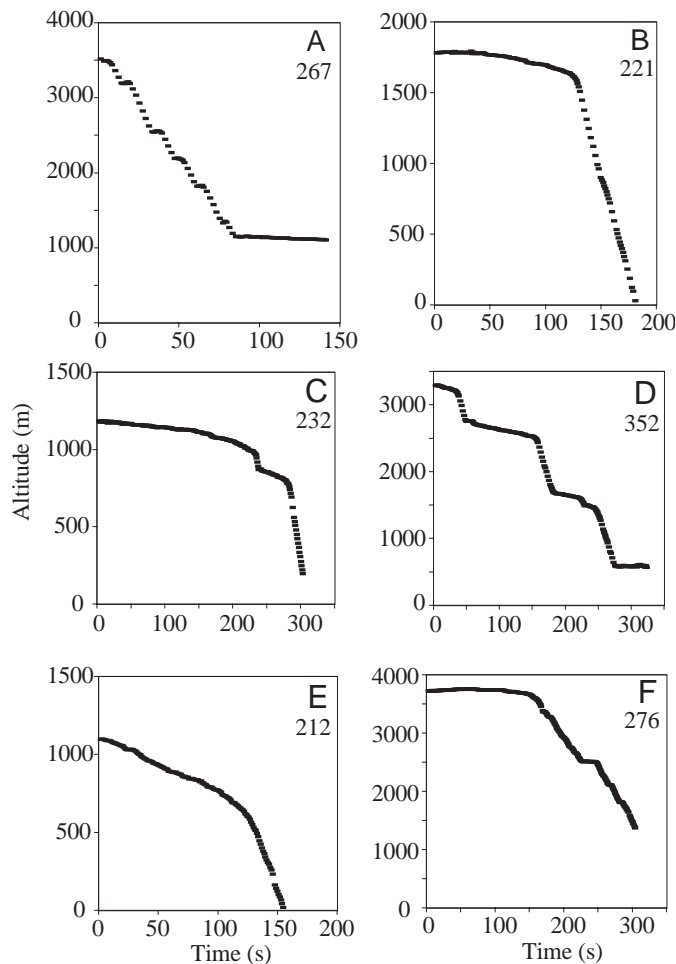
Fig. 1. Altitude *versus* time for passerine birds showing rapid descents during migratory flights as recorded by radar. On the basis of their wingbeat signature, the six tracks illustrated are referred to as (A) barn swallow, (B) yellow wagtail, (C) reed warbler, (D) yellow wagtail, (E) meadow pipit and (F) yellow wagtail. The numbers shown in each panel refer to the track identification number also given in Table 1.
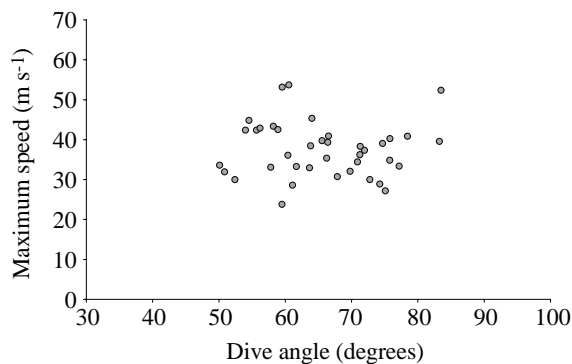

Fig. 2. Maximum airspeed along the flight path *versus* dive angle (horizontal=0 °) in 39 dive measurements of passerine birds tracked by radar. The maximum speeds refer to segments of tracks at least 4 s long. Each track is represented by only one such segment (see Table 1).
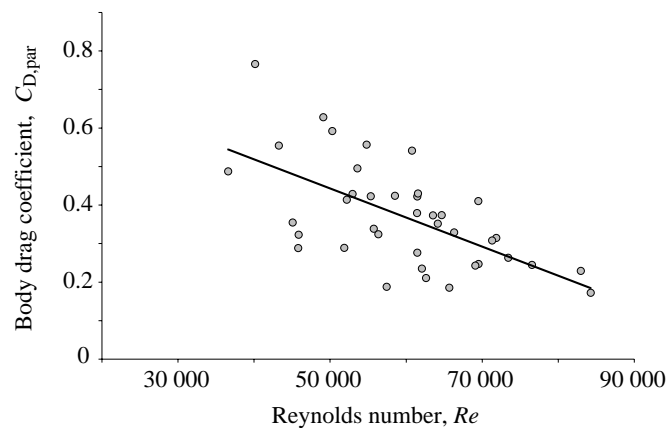
Fig. 3. Estimated body drag coefficients ($C_{D,par}$) *versus* Reynolds number (*Re*) for 39 dive measurements of passerine birds tracked by radar. Reynolds number was calculated using the diameter of the body frontal area as the reference length. The regression equation was $C_{D,par}=0.82-7.5\times10^{-6}Re$ (*t*=4.77, *P*<0.001).

Discussion

Diving speeds

We have presented radar tracks of migrating passerine birds commencing rapid descents from their cruising altitude. The birds were tracked during their spring migration, and the dives probably represent the termination of migration flights across the Mediterranean Sea. The bird with the steepest dive angle (83.5 °) reached a maximum speed of 52.3 m s^{-1}, which is near the maximum speed recorded at a lower dive angle for another bird (53.7 m s^{-1} at dive angle 60.6 °; bird 290). It seems that small birds can reach very high diving speeds, such as the maximum speeds recorded (>50 m s^{-1}), but that many birds control the speed of their dives by adjusting the positions of their wings and perhaps their legs to increase drag. This is supported by the strong correlation between the height at the midpoint of the dive and the dive speed, which might be caused by greater speed control at lower altitudes where the birds might head for a specific site to land. Any characteristic flight speed is expected to increase by approximately 5 % per 1000 m increase in altitude because air density decreases with altitude. This effect would cause a reduction in the mean dive speed (37.5 m s^{-1}) of approximately 1.9 m s^{-1} per 1000 m reduction in altitude, which is less than we observed (5.7 m s^{-1} per 1000 m change in altitude). Nevertheless, we believe that the maximum speeds achieved will represent situations in which the minimum possible drag will be exhibited. The mean and maximum diving speeds recorded are comparable with measurements of maximum diving speeds in larger bird species. For example, large falcons, famous for their stoops when attacking aerial prey, have been recorded as achieving top speeds in the range 39–58 m s^{-1} (Alerstam, 1987; Peter and Kestenholz, 1998; Tucker et al., 1998). Tucker et al. (Tucker et al., 1998) even mention preliminary measurements of speeds of 70 m s^{-1} in wild peregrines (*Falco peregrinus*)

that would represent the maximum speed ever measured for a bird using reliable methods. Our data refer to passerines, which are much smaller than the birds with the previously reported top speeds. Even if only a few dives achieved speeds in excess of $50\,\mathrm{m\,s^{-1}}$, this indicates that small birds also have the capacity to achieve very fast speeds when diving, and that the size of the bird has little or no effect on the maximum dive speed.

There is an expected size-dependent maximum glide/dive speed (e.g. Andersson and Norberg, 1981), but the available data lend little support to this prediction. We found no statistically significant (P=0.051) relationship between maximum speed and body mass within our data set of rather limited size range. The lack of such a relationship may not, however, be a critical rejection of the size-dependent maximum diving speed since birds may control their speeds below the theoretical maximum for other than aerodynamic reasons. Tucker (Tucker, 1998) derived theoretical top speeds for a falcon of $89–112\,\mathrm{m\,s^{-1}}$ with $C_{\mathrm{D,par}}$=0.18, and even up to $138–174\,\mathrm{m\,s^{-1}}$ for a $C_{\mathrm{D,par}}$ of 0.07. Not even the peregrine mentioned above achieved such high speeds.

Sources of error

Before discussing the body drag coefficients obtained, we will briefly discuss some potential sources of error that could have influenced the results. Identification of species was indirect because it was based on wingbeat signatures obtained from the radar echo signal. This method has been used before (e.g. Bloch et al., 1981) and, even if the species was wrong, the wingbeat frequency is strongly related to the size of the bird (Pennycuick, 1996). Recently, the radar wingbeat signatures of identified swallows and house martins (*Delichon urbica*) were found to agree with those obtained from the same species observed in a wind tunnel (L. Bruderer, personal communication). Track 267 was positively identified as a barn swallow, and that bird achieved the second highest diving speed recorded in an almost vertical dive.

Horizontal winds will affect the horizontal airspeed derived from the trackings and, hence, the estimated dive angles with respect to the air. We calculated the horizontal airspeeds on the basis of the mean wind speed measured before and after each bird track registration, separated by 4 h. We also calculated the horizontal airspeed on the basis of the first and second wind measurements separately, but the differences were quite small. Vertical winds were not measured, and rising thermals or sinking air could have affected the estimated vertical speeds. However, even in the tropics, where thermals are strong, they are of the order of $2–5\,\mathrm{m\,s^{-1}}$ (Pennycuick, 1998), which is small compared with the speeds measured for the birds when diving. In conclusion, there are a few potential sources of error, but they are not expected to be systematic and will not, therefore, influence the general conclusions of this study to any significant degree.

Values of $C_{\mathrm{D,par}}$

Our results gave values of $C_{\mathrm{D,par}}$ between 0.17 and 0.77,

with a mean of 0.37. The mean value is close to the 'old' default value for small passerines suggested by Pennycuick (Pennycuick, 1989). However, we suspect that some birds controlled their speeds below their potential maximum by increasing drag, resulting in some of the quite large values (>0.4). The gyrfalcon (*Falco rusticolus*) studied by Tucker et al. (Tucker et al., 1998) controlled its speed by changing the angle of attack of its cupped wings and by lowering its tarsi and feet from their normal position tucked up under the tail. Therefore, we think that some of the larger values (0.6–0.7) might be unrealistic for bird bodies, but that our mean estimate of $C_{\mathrm{D,par}}$=0.37 could be typical for passerines at cruising speeds. This is near the 'old' default value of 0.4, while our lowest values are close to the value of 0.24 obtained for frozen bodies of large birds measured in a wind tunnel (Pennycuick et al., 1988).

Tucker (Tucker, 1990) took great care when measuring a frozen peregrine body and obtained a $C_{\mathrm{D,par}}$ of 0.24; he also prepared a smooth surface model of the peregrine that gave a $C_{\mathrm{D,par}}$ of 0.14. Our lowest values are within this range, although our measurements refer to passerines. Pennycuick et al. (Pennycuick et al., 1996) arrived at even lower values for a thrush nightingale and a teal, using the speed of minimum wingbeat frequency and the calculated speed of minimum mechanical power. To get the two speeds to match, the calculated mechanical power curve was shifted by reducing $C_{\mathrm{D,par}}$ to 0.07. In a wind tunnel study of the mechanical power of a swallow (*Hirundo rustica*), Pennycuick et al. (Pennycuick et al., 2000) derived a novel method for estimating the mechanical power required to fly on the basis of the vertical accelerations of the body and the wingbeat kinematics during the course of a wingbeat. They did not, however, find close agreement between the speeds of minimum wingbeat frequency and estimated minimum power, which may question the assumption that these minima should coincide. Be that as it may, on the basis of our data, we may conclude that $C_{\mathrm{D,par}}$ for passerines used for calculating flight performance in birds (for example, by using the programs published by Pennycuick, 1989), should be of the order of 0.4 (the 'old' default value). We found no values as low as 0.1, the 'new' default value recommended by Pennycuick (Pennycuick, 1999), which is approximately half our lowest value (0.2; Fig. 3). One advantage of the present data is that they were obtained using a different method from those of previous studies, and yet we achieved surprisingly realistic values.

The negative correlation between $C_{\mathrm{D,par}}$ and Re shown in Fig. 3 illustrates a potentially interesting feature of the drag of bird bodies. At some critical value of Re, there is usually a transition from a laminar to a turbulent boundary layer, which is associated with a reduction in $C_{\mathrm{D,par}}$. In a circular cylinder, this transition occurs at approximately Re=300 000 (Anderson, 1991), but this point can be reduced to approximately Re=50 000 by mounting a thin wire just in front of the leading edge on model aircraft wings (Simons, 1994). Diving passerine birds may be operating in the zone of Re where turbulence in the boundary layer can be induced and used to reduce $C_{\mathrm{D,par}}$

(Pennycuick, 1989), although it remains to be demonstrated that this is the mechanism for real bird bodies. Passerine birds flying at typical cruising speeds (10–20 m s^{-1}) operate at $Re \approx 30\,000$, which is clearly below the range of Re of the diving birds (see Fig. 3). The lowest values of $C_{D,par}$ were found at $Re \geqslant 57\,000$, again suggesting that the 'old' default value of 0.4 could be typical of passerine birds in cruising flight.

The aerodynamic performance of passerine birds is certainly impressive, allowing them to migrate long distances, such as across the Sahara and the Mediterranean Sea, without refuelling. Changing $C_{D,par}$ to much lower values, as suggested by recent studies, will have quite dramatic consequences for our interpretation of flight performance (Pennycuick et al., 1996). For example, the lift to drag ratio will increase if $C_{D,par}$ is reduced and, hence, the potential flight range calculated on the basis of flight mechanical theory will increase. Also, characteristic flight speeds, such as those associated with minimum power, maximum range and maximum overall migration speeds (*sensu* Hedenström and Alerstam, 1995), will increase if $C_{D,par}$ is reduced. Because of the difficulties involved in challenging birds to minimise drag when diving in the field and methodological difficulties when studying birds in wind tunnels, we predict that the last word concerning body drag coefficients in birds has not yet been written.

List of symbols

b	wingspan
b_{max}	maximum wingspan
c	mean chord of wing
$C_{D,par}$	parasite drag coefficient
$C_{D,pro}$	profile drag coefficient
C_L	lift coefficient
D	drag
D_{ind}	induced drag
D_{par}	parasite drag
D_{pro}	profile drag
$\boldsymbol{g}$	acceleration due to gravity
k	induced drag factor
l	length, diameter of body
L	lift
m	body mass
Re	Reynolds number
S_b	body frontal area
S_{max}	maximum wing area
S_w	wing area
V	airspeed
V_{mp}	minimum power speed
V_s	sinking speed
$X, Y, Z,$	spatial coordinates
Z_1	start altitude of dive measurement
Z_2	stop altitude of dive measurement
Δt	time interval
θ	dive angle with respect to horizontal
μ	dynamic viscosity
π	ratio of circumference to diameter of a circle
ρ	air density
ν	kinematic viscosity

References

Alerstam, T. (1987). Radar observations of the stoop of the peregrine falcon *Falco peregrinus* and the goshawk *Accipiter gentilis*. *Ibis* **129**, 267–273.

Anderson, J. D., Jr (1991). *Fundamentals of Aerodynamics*. Second edition. New York: McGraw-Hill.

Andersson, M. and Norberg, R. Å. (1981). Evolution of reversed sexual size dimorphism and role of partitioning among predatory birds, with a size scaling of flight performance. *Biol. J. Linn. Soc.* **15**, 105–130.

Batchelor, G. K. (1967). *An Introduction to Fluid Dynamics*. Cambridge: Cambridge University Press.

Bloch, R., Bruderer, B. and Steiner, P. (1981). Flugverhalten nächtlich ziehender Vögel – Radardaten über den Zug verschiedener Vogeltypen auf einem Alpenpass. *Vogelwarte* **31**, 119–149.

Bruderer, B. (1997). The study of bird migration by radar. I. The technical basis. *Naturwissenschaften* **84**, 1–8.

Hedenström, A. and Alerstam, T. (1995). Optimal flight speed of birds. *Phil. Trans. R. Soc. Lond. B* **348**, 471–487.

Lide, D. R. (1997). (ed.) *CRC Handbook of Chemistry and Physics*. 78th edition. Boca Raton, FL: CRC Press.

McCormick, B. W. (1995). *Aerodynamics, Aeronautics and Flight Mechanics*. Second edition. New York: John Wiley & Sons.

Pennycuick, C. J. (1968). Power requirements for horizontal flight in the pigeon *Columba livia*. *J. Exp. Biol.* **49**, 527–555.

Pennycuick, C. J. (1975). Mechanics of flight. In *Avian Biology*, vol. 5 (ed. D. S. Farner and J. R. King), pp. 1–75. New York: Academic Press.

Pennycuick, C. J. (1989). *Bird Flight Performance: A Practical Calculation Manual*. Oxford: Oxford University Press.

Pennycuick, C. J. (1996). Wingbeat frequency of birds in steady cruising flight: new data and improved predictions. *J. Exp. Biol.* **199**, 1613–1618.

Pennycuick, C. J. (1998). Field observations of thermals and thermal streets and the theory of cross-country soaring. *J. Avian Biol.* **29**, 33–43.

Pennycuick, C. J. (1999). *Measuring Birds' Wings for Flight Performance Calculations*. Second edition. Bristol: Boundary Layer Publications.

Pennycuick, C. J., Hedenström, A. and Rosén, M. (2000). Horizontal flight of a swallow (*Hirundo rustica*) observed in a windtunnel, with a new method for directly measuring mechanical power. *J. Exp. Biol.* **203**, 1755–1765.

Pennycuick, C. J., Heine, C. E., Kirkpatrick, S. J. and Fuller, M. R. (1992). The profile drag of a hawk's wing, measured by wake sampling in a wind tunnel. *J. Exp. Biol.* **165**, 1–19.

Pennycuick, C. J., Klaassen, M., Kvist, A. and Lindström, Å. (1996). Wingbeat frequency and the body drag anomaly: wind-tunnel observations on a thrush nightingale (*Luscinia luscinia*) and a teal (*Anas crecca*). *J. Exp. Biol.* **199**, 2757–2765.

Pennycuick, C. J., Obrecht, O. O. and Fuller, M. J. (1988). Empirical estimates of body drag of large waterfowl and raptors. *J. Exp. Biol.* **135**, 253–264.

Peter, D. and Kestenholz, M. (1998). Sturzflüge von Wanderfalke *Falco peregrinus* und Wüstenfalke *F. pelegrinoides*. *Orn. Beob.* **95**, 107–112.

Rae, W. H. and Pope, A. (1984). *Low-speed Wind Tunnel Testing*. New York: John Wiley.

Rosén, M. and Hedenström, A. (2001). Gliding flight in a jackdaw: a wind tunnel study. *J. Exp. Biol.* **204**, 1153–1166.

Simons, M. (1994). *Model Aircraft Aerodynamics*. Third edition. Hemel Hempstead, UK: Argus Books.

Thomas, A. L. R. (1993). On the aerodynamics of birds' tails. *Phil. Trans. R. Soc. Lond. B* **340**, 361–380.

Tobalske, B. W., Peacock, W. L. and Dial, K. P. (1999). Kinematics of flap-bounding flight in the zebra finch over a wide range of speeds. *J. Exp. Biol.* **202**, 1725–1739.

Tucker, V. A. (1990). Body drag, feather drag and interference drag of the mounting strut in a peregrine falcon, *Falco peregrinus*. *J. Exp. Biol.* **149**, 449–468.

Tucker, V. A. (1998). Gliding flight: speed and acceleration of falcons during diving and pull out. *J. Exp. Biol.* **201**, 403–414.

Tucker, V. A., Cade, T. J. and Tucker, A. E. (1998). Diving speeds and angles of a gyrfalcon (*Falco rusticolus*). *J. Exp. Biol.* **201**, 2061–2070.

Vogel, S. (1994). *Life in Moving Fluids: The Physical Biology of Flow*. Second edition. Princeton: Princeton University Press.